Investigation of key parameters affecting the use of Ultra-High Performance Fiber Reinforced Concrete (UHPFRC) as strengthening material

Structures 62 (2024) 106257

Contents lists available at ScienceDirect

Structures

journal homepage: www.elsevier.com/locate/structures

Investigation of key parameters affecting the use of Ultra-High Performance Fiber Reinforced Concrete (UHPFRC) as strengthening material

Spyridon A. Paschalis [a,*], Andreas P. Lampropoulos [b]

[a] University of West London, St Mary's Road, Ealing, London W5 5RF, UK
[b] University of Brighton, Brighton BN2 4GJ, UK

ARTICLE INFO

Keywords:
UHPFRC
Strengthening Techniques
Effective Design
Numerical Analysis
Cost Reduction

ABSTRACT

The use of Ultra-High Performance Fiber Reinforced Concrete (UHPFRC) for strengthening applications is gaining increasing attention due to its advantageous mechanical and durability characteristics. However, the lack of design guidelines and code recommendations hinders the extensive use of UHPFRC in strengthening applications. The aim of the present study is to offer valuable insights regarding the effect of critical parameters on the performance of UHPFRC as a strengthening material. In this current research, experimental and numerical results have been used to evaluate the effectiveness of UHPFRC layers for the structural upgrade of existing Reinforced Concrete (RC) beams. Critical parameters such as the thickness of the additional layers, the connection at the old-to-new concrete interface, the mechanical performance of UHPFRC, and the amount of additional longitudinal reinforcement have been studied, and recommendations for the effective design of the strengthened elements, considering both performance and cost, are presented. The results of the present study indicate that the addition of steel bars with different diameters in the layer increased the load-carrying capacity by up to 183%. On the contrary, an increase of 5.8% in the load-carrying capacity was achieved when the RC beams had 30 mm layers, and an 18.1% increment was achieved for layers with a higher thickness of 70 mm. The assumption of perfect connection at the interface, which can be achieved with dowels at the interface, resulted in further enhancement of the load carrying capacity, which was found to be equal to 11.8% for the 30 mm layer and 35.3% for the 70 mm layer. An increment of the UHPFRC tensile strength of the strengthening layer from 11.5 MPa to 14 MPa resulted in a further increment of the load-carrying capacity by 8%.

1. Introduction

The structural safety of existing aging structures is an emerging field worldwide. A challenging issue is the structural upgrade of these structures using reliable techniques, which are also easy to apply. Some of the main disadvantages of traditional techniques are inadequate structural performance, difficulty in the application, disturbance in occupancy, and higher costs due to the expertise required for these techniques' applications. Strengthening using Ultra-High Performance Fiber Reinforced Concrete (UHPFRC) is a relatively new and promising technique with advantages over traditional methods.

Several studies in the literature focus on the mechanical properties of UHPFRC and the parameters affecting its performance. Abbas et al. [1] investigated the effect of fiber length and fiber content on the performance of the UHPFRC. They found that higher volumes of fibers result in higher tensile and flexural strength. Also, higher load-carrying capacity was observed with the use of short compared to long fibers.

Paschalis and Lampropoulos [2] investigated the effect of fiber content and curing time on the tensile characteristics of UHPFRC. They found that the tensile characteristics of the material change significantly for different fiber contents and different stress-strain models were proposed for different fiber volume fractions. In addition, they observed that steam curing for seven days results to strength values equivalent to the 90 days strength of ambient temperature cured UHPFRC.

Gesoglu et al. [3] investigated the effect of fiber type and fiber content on the performance of UHPFRC. In this study, fiber content of up to 2 vol% was investigated, as well as two types of fibers: hooked steel fibers and glass fibers. It was found that the tensile, compressive, and flexural strength increased with increasing steel-hooked fiber content. A decrease in strength was observed for fiber contents higher than 1.5 vol % in the case of glass fiber reinforcement.

Nicolaides et al. [4], conducted experimental work on the

* Corresponding author.
E-mail address: pascspy@uwl.ac.uk (S.A. Paschalis).

https://doi.org/10.1016/j.istruc.2024.106257
Received 1 May 2023; Received in revised form 8 March 2024; Accepted 18 March 2024
Available online 27 March 2024

Table 1
Description of the examined specimens.

Specimens ID	Number of specimens	Description
Beams B1	2	Initial RC beams (without extra layer)
Beams B2	2	RC Beams strengthened with 50 mm UHPFRC layer
Beams B3	2	Beams strengthened with 50 mm UHPFRC layer and dowels at the UHPFRC-to-RC interface.
Beams B4	2	Beams strengthened with 50 mm UHPFRC layer reinforced with additional steel bars.

development of UHPFRC using materials locally available in Cyprus and they proposed an optimum mix design. The mix design had a water-binder ratio of 0.16 and a fiber content of 6 vol%. The compressive strength of the mix was equal to 175 MPa and the fracture energy was 26.000 N/m. Kazemi et al. [5] investigated the properties of UHPFRC for steel fiber contents up to 5%, and they concluded that the higher fiber contents result in higher flexural and tensile strength.

The behaviour of UHPFRC under cyclic loading for different fiber contents was investigated by Paschalis and Lampropoulos [6]. This study proposed a constitutive model that can predict the material's behaviour under cyclic loading. In addition, a model for the degradation of the modulus of elasticity with the loading cycles was proposed. The orientation of fibers and the size of the elements can affect the performance of UHPFRC, and this has been highlighted in several studies [7–10].

UHPFRC has been applied in repair and strengthening applications. The strengthening of existing Reinforced Concrete column-to-beam joints is a challenging task due to the complexity of the application process when RC jackets or FRPS are used in addition to the demanding analytical calculation process. Tsonos and Kalogeropoulos [11] presented an analytical model for the prediction of the shear capacity of beam-column joints, which were strengthened with high-strength steel fiber-reinforced concrete and ultra-high performance fiber-reinforced concrete jackets. The proposed model was validated using experimental results of 50 beam-column joints as well as using data available in the literature. In this study, a modification coefficient factor was proposed to calculate the shear capacity of column-to-beam joints. Different values of the modification coefficient were proposed for Steel Fibre Reinforced Concrete (SFRC) with volume fraction values of 1% and 1.5%.

Tanarslan [12] applied UHPFRC in the form of laminate plates with a depth of 50 mm to strengthen under-reinforced RC beams. Both epoxy and mechanical bonding were used for the connection of the existing member with the new layer. In all cases, the maximum load-carrying capacity was increased, and it was found to be in the range of 32–208%. The disadvantages of the examined technique using prefabricated UHPFRC laminates were the quality control and the difficulty in the application.

Lampropoulos et al. [13] conducted an experimental study to identify the properties of UHPFRC. They developed a numerical model that can predict the performance of UHPFRC for the flexural strengthening of RC beams. The results indicated the effectiveness of the examined technique and superior properties compared to conventional techniques, such as strengthening with RC layers.

Dagenais and Massicotte [14] investigated the performance of lap splices, which were strengthened with UHPFRC under cyclic loading. In this study, six beams were examined in total, and UHPFRC replaced the concrete using different fiber contents. The results indicated that fiber content is a crucial parameter and can provide enhanced structural performance of lap-spliced load bearing elements.

Murthy et al. [15] applied thin UHPFRC layers of 10 mm to repair damaged RC beams. They identified an increase in the repaired beam's performance, and the failure mode was similar to that of the control beams without any extra layer.

Yin et al. [16] investigated the performance of UHPFRC for strengthening of RC slabs. Slabs with dimensions 1.6 m * 0.3 m strengthened with UHPFRC using different depths and configurations. The results indicated the effectiveness of the examined technique. Strengthening with UHPFRC resulted in reduction of diagonal cracks and better performance in the post elastic region with strain hardening and high energy absorption.

Al-Osta et al. [17] investigated the flexural performance of RC beams, which were strengthened with UHPFRC. In this investigation, two different strengthening techniques were investigated: using sand blasting and in-situ UHPFRC, and by bonding pre-fabricated strips. The results indicated that both techniques were effective, but the sand-blasting technique presented a superior performance overall.

Safdar et al. [18], conducted experimental and numerical investigation on the performance of UHPFRC as a repair material. RC beams were repaired in both tension and compression zones using UHPFRC with different layers, and the repaired elements were tested under four-point flexural testing. The results indicated that the flexural strength of the elements was increased for higher thicknesses. In this study, it was concluded that UHPFRC improves mainly the stiffness of the repaired beams.

Bruhwiler and Denarie [19] applied UHPFRC in real-life applications. In the first application, the researchers retrofitted the kerbs of a bridge using prefabricated UHPFRC. The mechanical properties were validated with uniaxial tests, and the low permeability, which is essential for this type of application, was confirmed using permeability tests. The researchers also presented the construction of a crash barrier on a highway bridge using UHPFRC. Apart from high strength and low permeability, this application required protection from impact, which is one of the main advantages of UHPFRC. In another application, the researchers applied UHPFRC for the retrofitting of a bridge pier using prefabricated UHPFRC layers. Epoxy was used to connect the new element with the existing one. Finally, in this study, the application of UHPFRC for the strengthening of an industrial floor was presented. Some advantages of this application over traditional techniques were the excellent mechanical properties of UHPFRC and the good workability.

Yoo et al. [20], investigated the effect of crack repair using epoxy sealing on the tensile behaviour of UHPFRC under a corrosive environment and for different crack widths. This study found that for small crack widths (0.1 mm), the tensile characteristics of UHPFRC changed slightly. However, the tensile strength was increased significantly for higher crack widths (>0.3 mm).

Elsayed et al. [21] investigated experimentally the behaviour of RC Columns strengthened with UHPFRC under eccentric loading. The experimental results indicated that strengthening with UHPFRC is an effective technique resulting in higher strength, stiffness, moment capacity, and toughness. Also, it was found that the increase in axial load carrying capacity, the moment capacity, and the stiffness is inversely proportional to the load eccentricity ratio.

The interface connection between UHPFRC and RC is an important parameter that should be considered for the design of strengthening techniques using UHPFRC [22,23]. It has been found that despite the better connection between UHPFRC and RC, compared to concrete-to-concrete interfaces, the slips are not negligible, and high values have been recorded in the post-elastic phase [22]. Dowels at the interface between UHPFRC and concrete reduce the interface slips and result in higher load-carrying capacity [23].

Based on studies in the literature, the application of UHPFRC for strengthening purposes presents advantages, including ease of application, enhanced structural performance and ductility, and the small thickness of the applied layers/jackets.

Strengthening existing structures using Ultra-High Performance Fiber Reinforced Concrete (UHPFRC) is a promising technique with advantages over traditional methods such as strengthening with Reinforced Concrete (RC) layers and jackets. However, for the effective

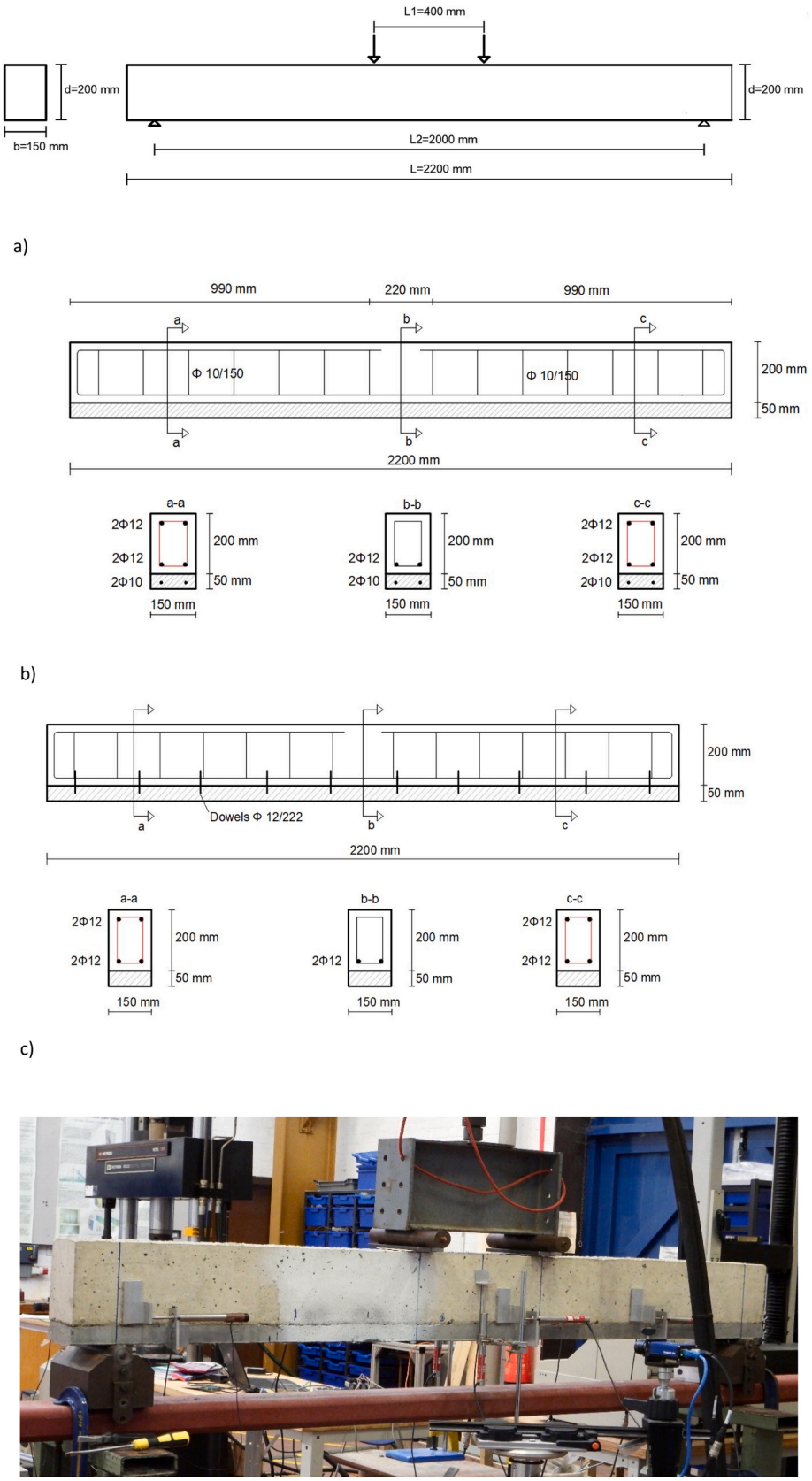

Fig. 1. d)
a) Loading conditions and dimensions of the control beam b) Dimensions of the strengthened beams with layers and bars c) Dimensions of strengthened beams with layers and dowels d) Beam ready for testing.

Table 2
UHPFRC mix design [22].

Material	Mix proportions (kg/m^3)
Cement	620
GGBS	434
Silica fume	140
Silica Sand	1051
Superplasticizer	59
Water	185
Steel fibers	235.5 (3%Vol.-%)

design of the strengthening scheme, parameters including the layer depth, the amount of steel fibers, the use of steel bars in the layers, and the interface conditions should be taken into consideration. From the literature there is a lack of systematic studies on the effective design of strengthening techniques using UHPFRC considering parameters such as structural performance and cost. In the present study, the results of experimental tests have been used, in addition to a parametric numerical study, to investigate the effect of these critical parameters on the structural performance of UHPFRC-strengthened elements. The aim of the present study is to offer valuable insights regarding the impact of essential parameters on the performance of UHPFRC-strengthened elements and assist practitioners, designers, and researchers with the design process and with the selection of the optimum UHPFRC characteristics considering both the performance and the cost.

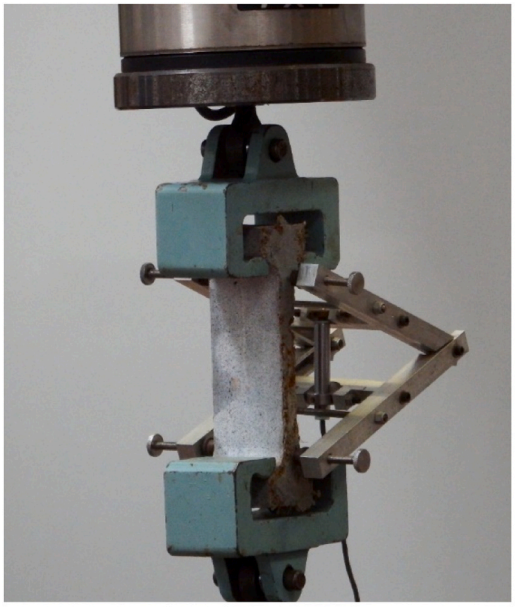

a)

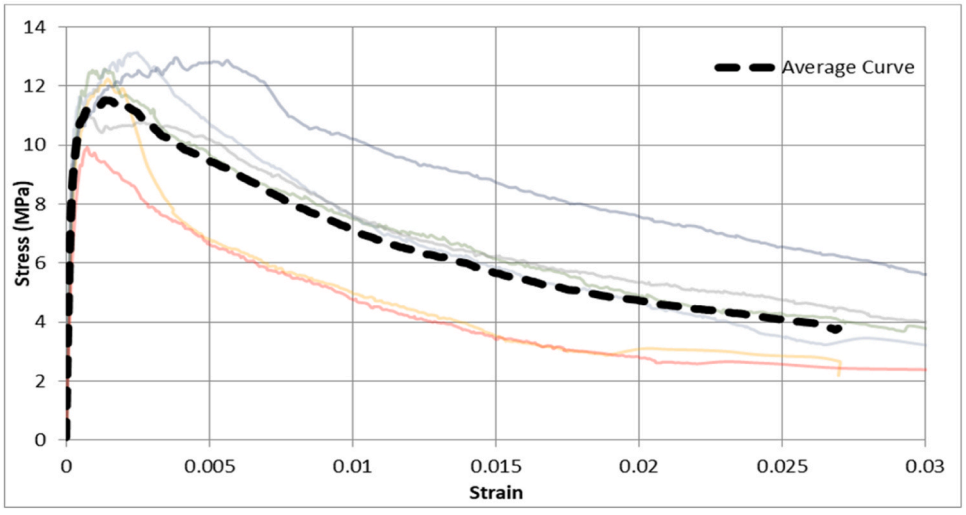

b)

Fig. 2. a) Dog Bone specimen b) Experiment results from the testing of UHPFRC in tension.

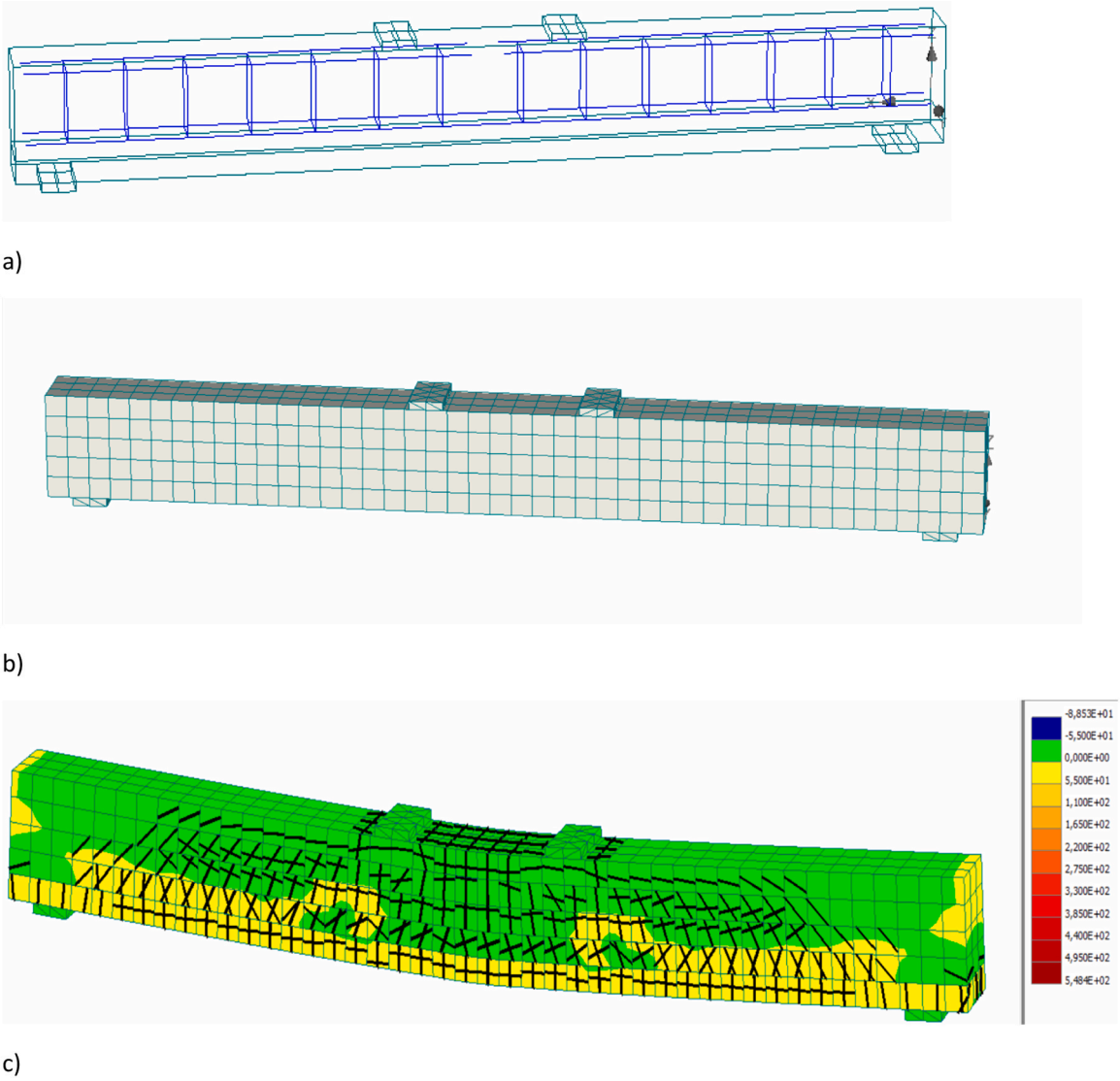

Fig. 3. a) Geometrical Model used in the Finite Element Analysis b) Mesh generation c) crack pattern and stresses for an examined beam.

Table 3
Values used in the numerical modelling.

Compressive strength of concrete	30.9 MPa
Compressive strength of UHPFRC	137 MPa
Tensile strength of UHPFRC	11.5 MPa
Cracking stress of UHPFRC	5 MPa
Modulus of Elasticity of UHPFRC	51 GPa
Coefficient of friction	0.98
Cohesion	1.8 MPa
Yield Stress of steel	500 MPa
Shrinkage	565 microstrain

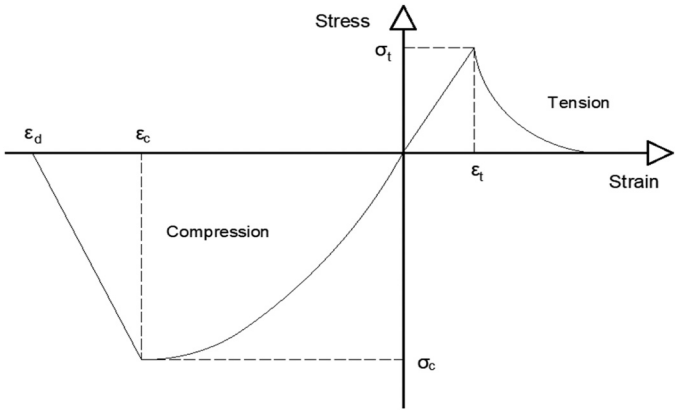

Fig. 4. Modelling of Concrete.

2. Experimental and numerical program

2.1. Tested beam

In the present research, experimental results from the testing of Reinforced Concrete (RC) beams have been used to develop a numerical model that can predict the response of strengthened elements with UHPFRC layers.

In the experimental study, different configurations were examined. The four main types of specimens consisted of i) control RC beams without strengthening, ii) RC beams strengthened with UHPFRC layers only, iii) RC beams strengthened with UHPFRC layers and dowels at the interface and iv) RC beams strengthened with UHPFRC layers with steel bars (Table 1).

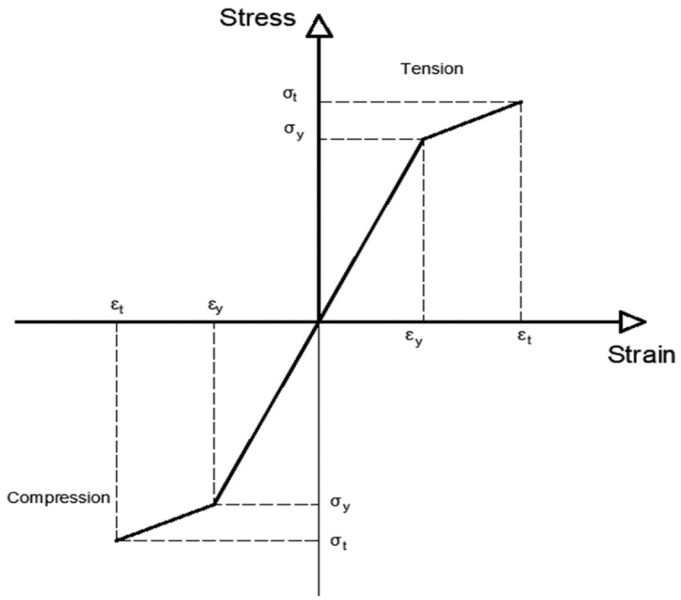

Fig. 5. Modelling of Steel Bars.

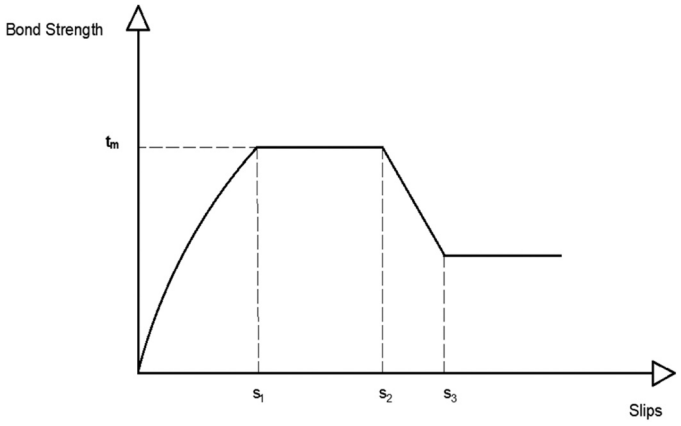

Fig. 6. Bond strength-slip law [21].

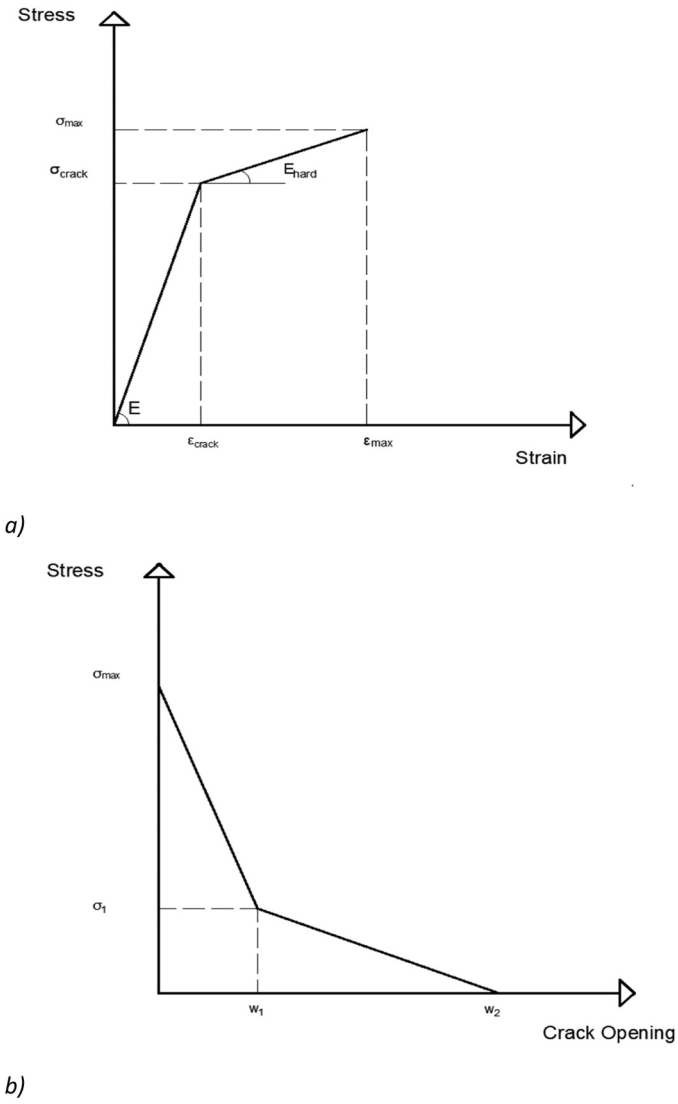

Fig. 7. Tensile behaviour of UHPFRC adopted in Atena a) Up to maximum stress b) after the maximum stress level.

Fig. 1a-d presents the configuration of the experimental investigation's beams. Compared to the modelling values for full-scale beams used by Noor and Boswell [24] (a width of 0.3 m, a depth of 0.45 m, and a length of 5 m), the beam of the present investigation can be considered half-scale.

The aim of the present investigation is the flexural strengthening of the beams. The beams were designed to be relatively weak in bending, with a lower depth-to-width ratio, and shear reinforcement was placed to ensure that the beam would not fail in shear.

As shown in Fig. 1, stirrups were placed along the length of the beam to avoid shear failure. All layers had a depth of 50 mm and were cast along the entire length of the beam. Before applying the layers, the surface of the RC beams was roughened to a depth of 2–2.5 mm. The depth was measured using the sand patch method [22]. On the other hand, the steel bars in the layers had a diameter of 10 mm. The RC beams were reinforced at the tensile side only, with two continuous steel bars with a diameter of 12 mm to represent substandard RC beams. The steel bars at the top were placed to facilitate the construction of the shear links.

The geometry, the reinforcement and the loading conditions of this study were selected in agreement with a previous research programme where RC beams were strengthened with conventional RC layers [25], leading to comparable conclusions for the different techniques [26]. Also, parameters such as the reinforcement ratio of the present study are in accordance with existing studies investigating strengthening techniques for existing RC members ([12], [27], [28]).

High shear stresses are expected at the interface between UHPFRC and RC, and different types of failure of the mechanical connectors (dowels) may occur, such as a failure of concrete, a failure of steel, and concrete cone failure. The design of dowels was based on the Greek Retrofitting Code [29]. Ribbed steel bars of 12 mm diameter were used as dowels, with 126 mm length, embedment length of 96 mm, and spacing of 222 mm (Fig. 1). The selected characteristics align with the recommendations for embedment length at least eight times the diameter of dowels. The cover in the direction of loading should be at least five times the diameter of the dowels to prevent premature failure of the concrete edges around the dowels. The dowels were inserted in the beam using a thixotropic structural two-part adhesive, considering technical specifications [30], and the diameter of the hole was 4 mm bigger than the diameter of the dowels.

A four-point loading test was adopted to test the examined beams, allowing a uniform distribution of the stresses in the middle of the span where there is a constant bending moment distribution without shear forces. The beams were tested under a displacement rate of 8 μm/s,

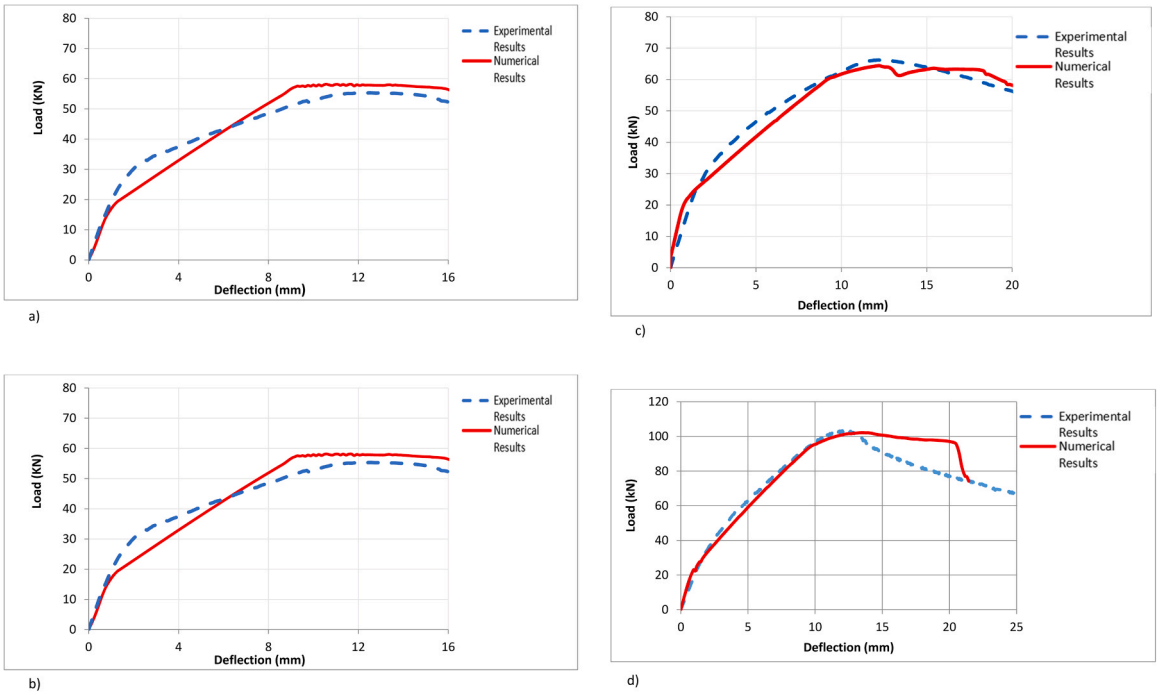

Fig. 8. Comparison between experimental and numerical results for a) the control beam b) the beam strengthened with UHPFRC layer c) the beam strengthened with UHPFRC layer and dowels d) the beam strengthened with UHPFRC layer and additional steel bars.

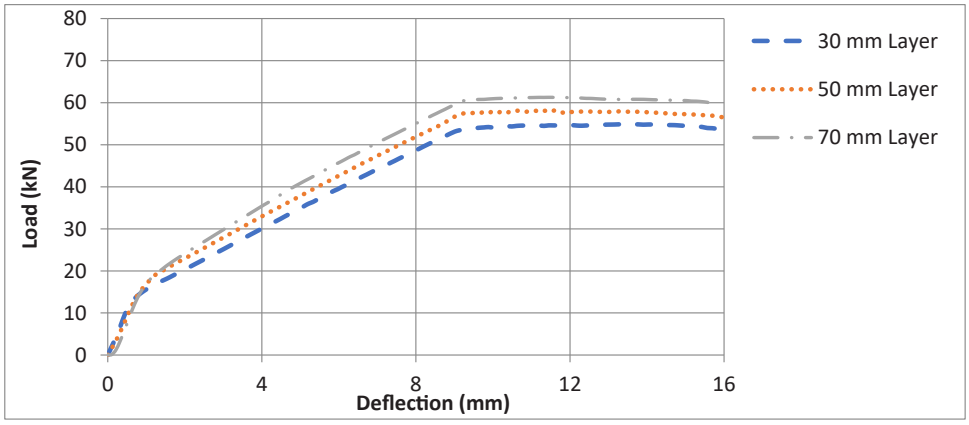

Fig. 9. Load carrying capacity for different layer depths.

which is in line with the loading rate used in a previous study [25] on evaluating the response of RC beams strengthened with additional RC layers.

It must be mentioned here that the present study focuses on strengthening RC beams. In the case of existing substandard RC structures, the strengthening of the beam-to-column joints, in addition to the jacketing of the existing columns, should be considered to prevent any failures at the joints and/or at the columns. An issue when increasing the flexural capacity of beams is the shear failure of the beams. UHPFRC jackets could be used to avoid shear failure of beams. Also, the combination of UHPFRC with FRPs could be considered.

2.2. Properties of the materials

For the preparation of UHPFRC cement, 52.5 R was used together with fine sand with a maximum size of 0.5 mm, Ground Granulated Furnace Slag, Silica Fume, Superplasticizer, and fiber content of 3 vol% as can be seen in Table 2 [22]. The steel fibers had a diameter of 0.16 mm, length of 13 mm, tensile strength of 3000 MPa, and modulus of elasticity of 200 GPa.

All steel bars in the present investigation were B500C with a yield stress of 500 MPa, the ratio of the maximum tensile stress to the yield stress was 1.15, an elongation at the maximum load equal to 7.5%, and modulus of elasticity of 200 GPa [31].

To identify the compressive strength of concrete and UHPFRC cubes were tested based on BS EN to BS EN 12390–3:200 9 [32]. The compressive strength of UHPFRC was 137 MPa, and the standard deviation was 5.6 MPa. The average compressive strength of concrete cubes was 30.9 MPa, and the standard deviation was 2.3 MPa. According to BS EN 206–1 [33], considering 5% defective, the factor k equals 1.64. Therefore, the characteristic strength of the cube was 27 MPa, and the characteristic of the cylinder was 22 MPa. Based on this, concrete can be classified as C 20/25, a relatively low value which can be found in old structures. Considering durability and strength requirements, using concrete class higher than C 30/37 is recommended for new structures [34]. The mean value of the compressive strength in the existing study is

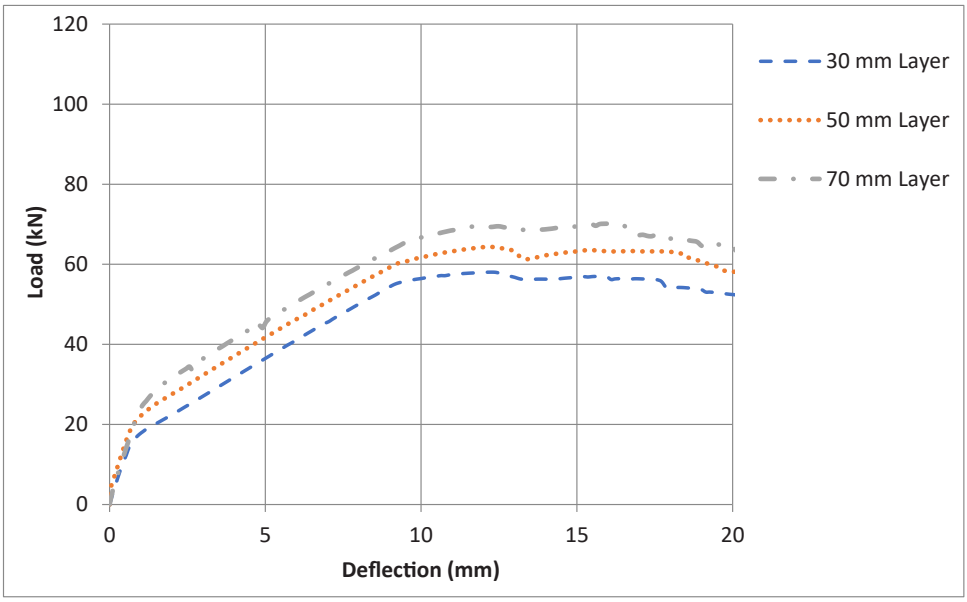

Fig. 10. Load-deflection curve for monolithic connection and different layer depths.

Table 4
Performance of strengthened beams for different layer depths and interface conditions.

Beam	Cracking Load (kN)-Numerical	Increase % Numerical (Compared to Initial Beam)	Cracking Load-Experimental Results (kN)	Maximum Load (kN)-Numerical	Increase % Numerical (Compared to Initial Beam)	Maximum Load-Experimental Results (kN)
Control Beam f_c	10.0		8.7	51.9		54.6
30 mm Non-monolithic	12.8	28.0		54.9	5.8	
30 mm Monolithic	15.9	59.0		58.0	11.8	
50 mm Non-monolithic	15.3	53.0	15.5	58.2	12.1	55.3
50 mm Monolithic	21.9	119.0	23.5	64.4	24.1	66.2
70 mm Non-monolithic	17.7	77.0		61.3	18.1	
70 mm Monolithic	24.9	149.0		70.2	35.3	

also in accordance with most existing studies in strengthening structures. Several studies exploring techniques of RC beams have reported mean compressive strength values for concrete within the range of 27 MPa-54 MPa ([17], [18], [21], [35], [36], [37]).

Concrete strength is an essential aspect as the interface cohesion is directly affected by the concrete strength of the weaker of the two concretes of the interface. In this case, the actual strength values should be considered for any concrete strength values. The shear strength characteristics at the interface need to be calculated each time using the analytical models proposed in the relevant code provisions for the cohesion (which is directly linked to the concrete strength) and for the friction [38].

For the investigation of the tensile characteristics of UHPFRC dog bone specimens were prepared and tested under a displacement rate of 7 μm/sec (Fig. 2a). To measure the extension of the dog bone specimens on both sides during the testing, a Linear Variable Differential Transformer (LVDT) was placed on a steel frame which was attached to the dog bone specimens as can be seen in Fig. 2a. Specimens in which the failure occurred close to the grips were discarded. The dog bone specimens' geometry and the loading conditions are based on previously published studies in UHPFRC, leading to comparable results ([2], [6]).

Based on the results of Fig. 2, the maximum average tensile strength was 11.5 MPa, and the modulus of elasticity was 51 GPa.

2.3. Finite element modelling

For the numerical investigation, the finite element analysis software ATENA was used [39]. There are different options for mesh generation. For macro elements with six boundary surfaces, the mesh can only consist of brick elements. For other macro elements, tetrahedral or mixed meshes can be created. Brick elements were used for the beams while tetrahedral elements were used for the steel plates. As for the bending, it is recommended that at least four elements along the cross-section height should be used [39]. A mesh size of 0.05 m was used in this study (Fig. 3).

The material properties used in the numerical modelling were based on the experimental testing of materials, as presented in Section 2.2. Therefore, a value of 137 MPa was used as the compressive strength of UHPFRC, and a value of 30.9 MPa was used as the compressive strength of normal concrete. The average results of Fig. 2 were used to model the tensile characteristics of UHPFRC. The initial cracking occurred at a 5 MPa stress value, while the maximum stress was 11.5 MPa. The modulus of elasticity was calculated from the stress-strain graph and was taken equal to 51 GPa. The yield stress of steel bars was equal to 500 MPa. The interface connection between UHPFRC and RC was modeled using two-dimensional elements. In the present study, and for non-monolithic connection, the results of push-off tests of UHPFRC to RC interfaces from a previous experimental study [22] were used. Based

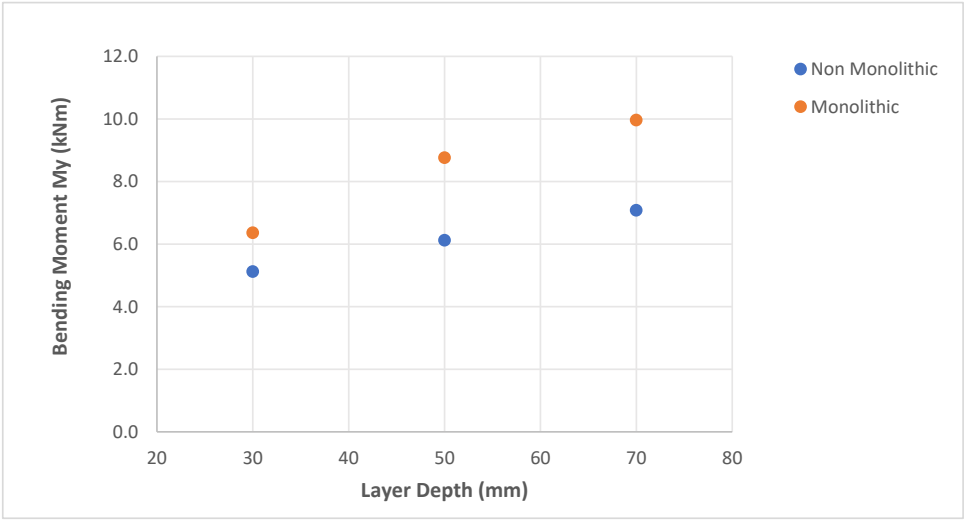

a)

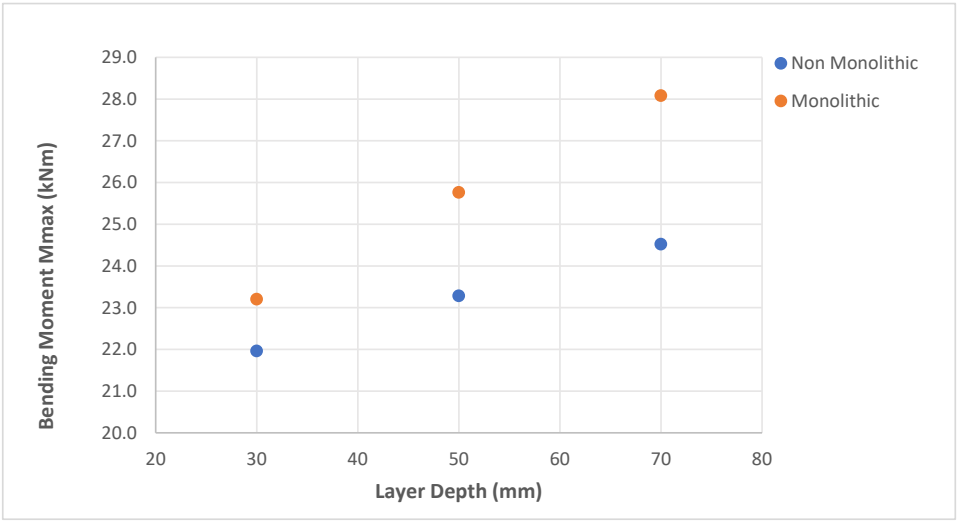

b)

Fig. 11. Bending Moment for the different interface conditions and layer depths at a) yield and b) maximum load.

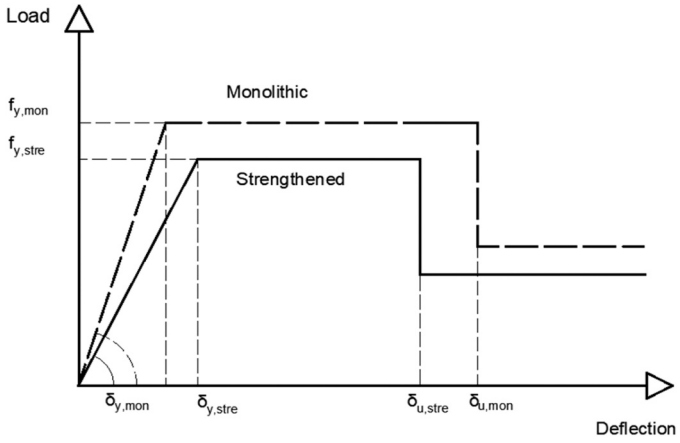

Fig. 12. Typical behaviour of a monolithic beam versus a strengthened beam [22].

on these results, a value of 0.98 was used for the coefficient of friction and a value of 1.8 MPa for cohesion. The effect of concrete shrinkage was also considered in the present investigation, and the shrinkage strain value was taken equal to 565 microstrains. This value was based on previous experimental measurements [2].

Table 3 summarises the values used for the numerical modelling.

For the modelling of concrete, the SBETA constitutive model [39] was adopted with non-linear behaviour in compression and tension (Fig. 4). In compression, the ascending branch is based on the CEB-FIP model [40], and the softening law is assumed to be linearly descending. In tension, a linear branch was assumed, followed by a second softening phase.

A bi-linear behaviour with hardening was assumed for the modelling of steel bars (Fig. 5).

For the analysis, the bond-slip law, according to the CEB-FIB [40], was adopted (Fig. 6).

The tensile behaviour of UHPFRC was modeled considering the experimental results of direct tensile tests (Fig. 2) and considering strain hardening behaviour as illustrated in Fig. 7a. The post-peak behaviour of

the material was modelled with a bi-liner model (Fig. 7b).

2.4. Validation of the numerical model

In the experimental investigation, two beams were tested for each configuration B1, B2, B3, and B4 (Table 1), and the average of two was considered. A comparison between the average experimental results and the numerical results is presented in Fig. 8a-d, respectively.

Three different phases can be identified in these graphs for all the examined cases. The first is the elastic uncracked region, and the second is the post-elastic part. In the second stage, cracks initiate, leading to reduced stiffness while the bridging effect of steel fibers is activated. Finally, in the third phase, yielding of the reinforcement occurs, with subsequent increased deformation, extensive cracking in the tensile side, and steel fibers pull out, followed by concrete crushing and reduction of the load-carrying capacity.

A good agreement was achieved between the experimental and the numerical investigations in all the examined cases. The load carry capacity of the control beam (Fig. 8a) of the numerical investigation was 95% of the experimental investigation. For the beams that were strengthened with UHPFRC layers only (Fig. 8b), the average maximum load-carrying capacity in the experimental investigation was 95% of the corresponding value in the numerical investigation.

In Fig. 8c, an excellent agreement was identified between the experimental results for the beams, which were strengthened with UHPFRC layers and dowels at the interface, and the numerical results considering a monolithic connection at the interface. In this case, the maximum load-carrying capacity of the beam of the numerical investigation was 97% of the load-carrying capacity of the experimental investigation.

Finally, a good agreement regarding maximum load-carrying capacity can be observed between the experimental and numerical results for the beams strengthened with UHPFRC layers and steel bars (Fig. 8d). More specifically, the maximum load-carrying capacity of the beam of the numerical investigation was 98.6% of the load-carrying capacity of the beam of the experimental investigation. In the experimental investigation, a steep decrease in the load-carrying capacity of the beam can be observed after reaching the maximum load-carrying capacity. This is due to the sudden failure of the compressive side of the beam in the post-peak area.

Table 6
Performance of strengthened beams for different interface conditions.

Layer Depth	K_k	K_r	$K_{\theta,y}$	$K_{\theta,u}$
30 mm	0.94	0.95	1.17	0.89
50 mm	0.69	0.9	1.19	0.87
70 mm	0.7	0.88	1.3	0.71

3. Parametric study on parameters affecting the performance of UHPFRC as strengthening material

3.1. Use of different layer depths

An advantage of applying UHPFRC as a strengthening material is that thin elements with high strength and ductility can be constructed. The layer depth is a crucial decision that must be considered for the technique's design. The geometry of existing members, the performance of the strengthened members, and the cost are crucial parameters that should be considered when selecting the appropriate layer depth.

Another critical parameter for the mechanical characteristics at the material level is the orientation and distribution of fibers. Commonly used fibers for UHPFRC are steel microfibers with a diameter of 0.16 mm and lengths of 9 mm and 13 mm. To avoid issues with the distribution of fibers, it is suggested that the thickness of UHPFRC elements should be higher than three times the length of the fibers. Therefore, the minimum required depth should be approximately 30 mm. Also, lower depths are impractical and are not expected to contribute significantly to the strengthened elements' load-bearing capacity. However, the distribution of fibers in thick elements (>70 mm) is an issue, and based on existing studies, there is a size effect that should be taken into consideration [7,10]. Considering all the above, layer depths using UHPFRC are suggested to be 30–70 mm.

In the present investigation, three different layer depths have been investigated: 30 mm, 50 mm, and 70 mm for the same fiber content (3 vol%). The numerical results are presented in Fig. 9.

The results of Fig. 9 indicate that the layer's depth affects the strengthened beams' performance. The maximum load of the beam with a 30 mm layer was 54.9 kN, while the load-carrying capacity of the beams with a 50 mm layer and a 70 mm layer were 58.2 kN and 61.3 kN, respectively. Based on these results, an increase of 12% in the load-carrying capacity was identified when the layer depth was

Table 5
Monolithicity coefficients.

$$K_r = \frac{f_{y,stre}}{f_{y,mon}} \quad (1)$$

where $f_{y,stre}$ is the resistance of the strengthened member and $f_{y,mon}$ is the resistance of the monolithic member.

$$K_k = \frac{K_{stre}}{K_{mon}} \quad (2)$$

where K_{stre} is the stiffness of the strengthened member and K_{mon} is the stiffness of the monolithic member.

$$K_{\theta,y} = \frac{\delta_{y,stre}}{\delta_{y,mon}} \quad (3)$$

where $\delta_{y,str}$ is the deformation of the strengthened beam at the yield load and $\delta_{y,mon}$ is the deformation of the monolithic beam at the yield load.

$$K_{\theta,u} = \frac{\delta_{u,stre}}{\delta_{u,mon}} \quad (4)$$

where $\delta_{u,stre}$ is the deformation of the strengthened beam at the maximum resistance and $\delta_{u,mon}$ is the deformation of the monolithic beam at the maximum resistance.

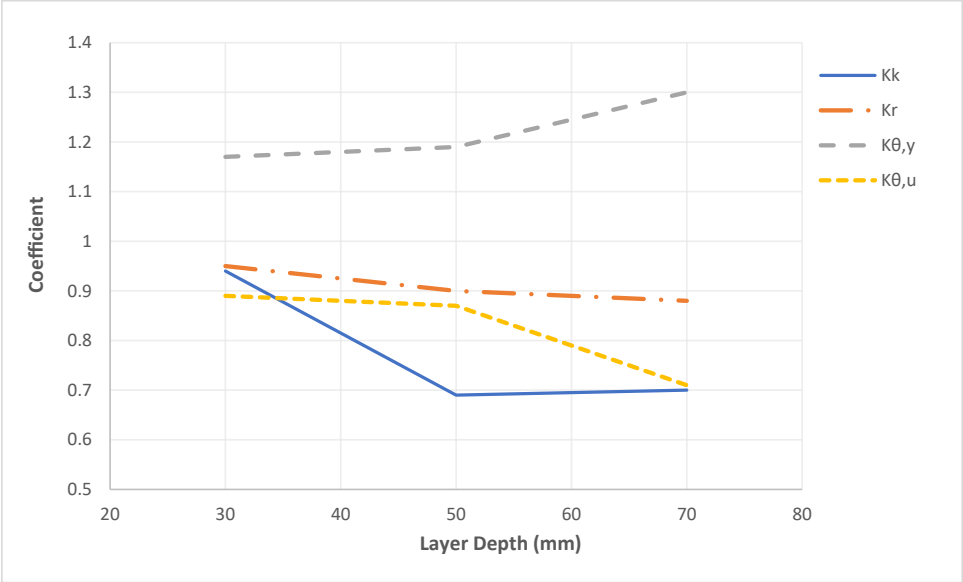

Fig. 13. Variation of the different coefficients for different layer depths.

increased from 30 mm to 70 mm.

The initiation of cracking in the strengthened beam was observed at 12.8 kN for the 30 mm layer, while for the 50 mm and 70 mm layers, cracking started at 15.3 kN and 17.7 kN, respectively. Additionally, the stiffness of the strengthened beams increased as the layer thickness increased. Specifically, the stiffness of the beams strengthened with 30 mm, 50 mm, and 70 mm layers was 18.4 kN/mm, 18.6 kN/mm, and 19 kN/mm, respectively.

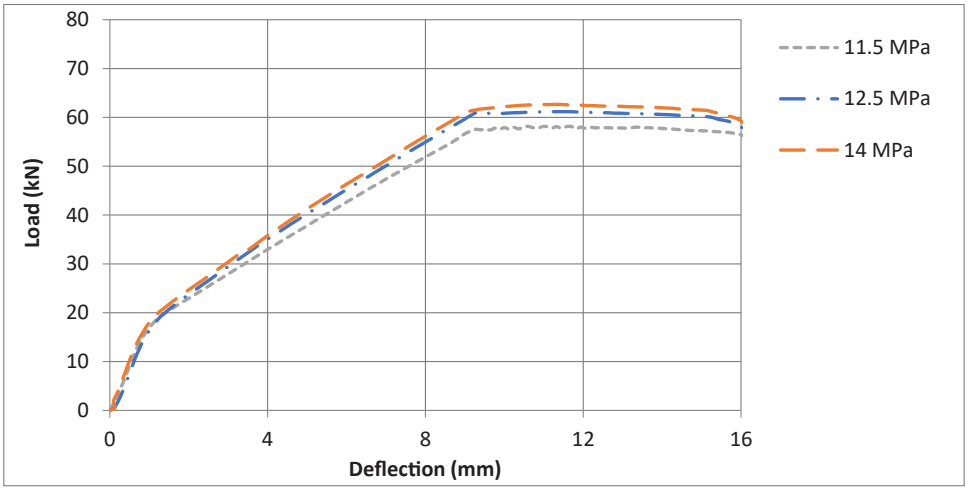

Fig. 14. Load carrying capacity for different tensile strengths.

Table 7
Result for various tensile characteristics.

	Cracking Load (kN)-Numerical	Increase % Numerical (Compared to Initial Beam)	Cracking Load (kN) Experimental	Maximum Load (kN) Numerical	Increase % Numerical (Compared to Initial Beam)	Maximum Load (kN) Experimental
Initial Beam	10.0		8.7	51.9		54.6
Layer 11.5 MPa Tensile strength	15.3	53.0	15.5	58.2	12.1	55.3
Layer 12.5 MPa Tensile Strength	17.1	71.0		61.2	17.9	
Layer 14.0 MPa Tensile Strength	18.5	85.0		62.7	20.8	

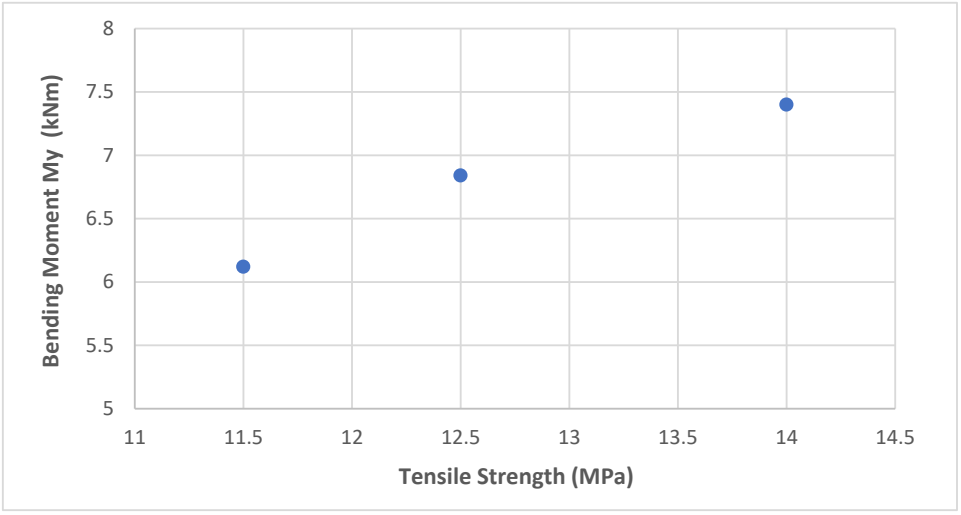

a)

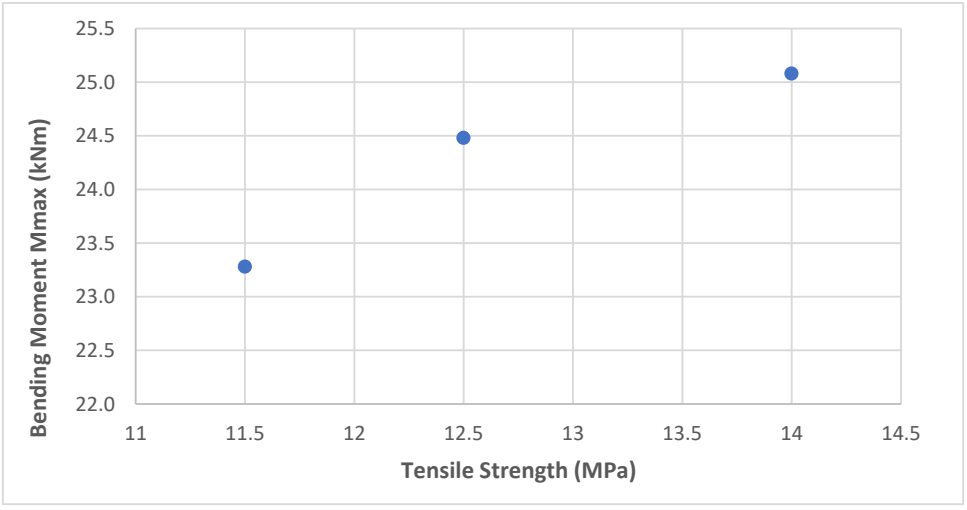

b)

Fig. 15. Bending Moment at a) yield b) max.

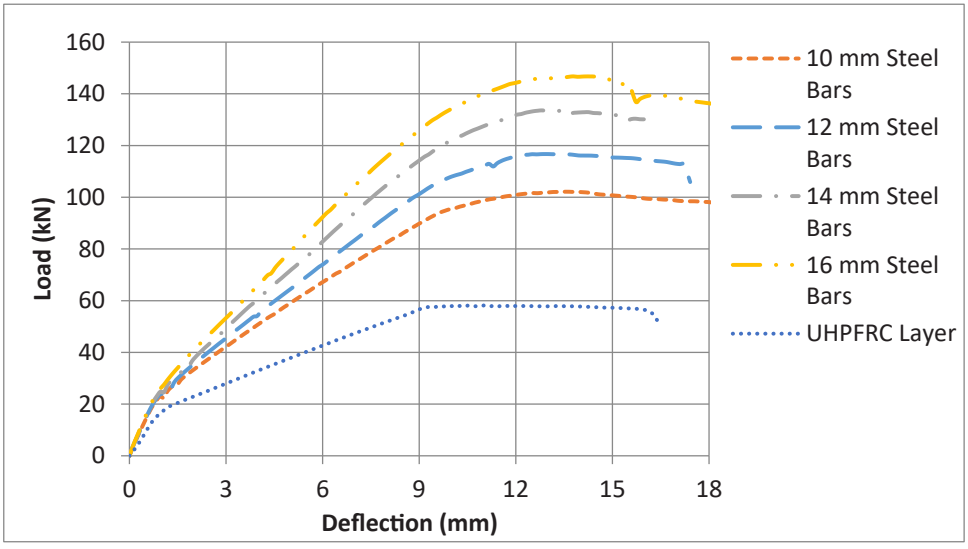

Fig. 16. Strengthening using different amounts of reinforcement in the layers.

Table 8
Effect of different amount of reinforcement in the layer.

Specimen	Cracking Load (kN)- Numerical	Increase % Numerical (Compared to Initial Beam)	Cracking Load (kN) Experimental	Maximum Load (kN) Numerical	Increase % Numerical (Compared to Initial Beam)	Maximum Load (kN) Experimental
Initial Beam	10.0		8.7	51.9		
Layer without bars	15.3	53.0	15.5	58.2	12.0	55.3
Layer and 10 mm bars	23.1	131.0	27	102.1	97.0	103.4
Layer and 12 mm bars	23.8	138.0		116.7	124.0	
Layer and 14 mm bars	24.8	148.0		133.7	158.0	
Layer and 16 mm bars	27.5	175.0		146.8	183.0	

3.2. Effectiveness of different layer depths considering a monolithic connection

The connection between UHPFRC and concrete is better compared to concrete-to-concrete interfaces [22] with lower interface slips, and many researchers have eliminated the use of dowels. However, according to the latest research, the slips at the interface between UHPFRC and concrete are not negligible, and the use of dowels results in a connection that approaches the monolithic [23].

The present section aims to investigate the performance of strengthened beams with different layer depths considering the monolithic connection at the interface, which can be achieved with the use of dowels [23]. The load-deflection results for different layer depths and monolithic connection at the interface are presented in Fig. 10.

Based on the results of Fig. 10, the maximum load-carrying capacity of the strengthened beam with a 30 mm layer was 58.1 kN, while the values for the 50 mm and 70 mm layers were 64.4 kN and 70.2 kN, respectively. These results show that when the layer depth is increased from 30 mm to 70 mm, the load-carrying capacity increases by almost 21%.

Apart from the load carrying capacity, the stiffness of the strengthened beams was increased for increasing layer depths. More specifically, for layer depths 30 mm, 50 mm, and 70 mm, the stiffness was equal to 22.8 kN/mm, 23.6 kN/mm, and 24.4 kN/mm, respectively. Finally, for increasing layer depths, the cracking was also delayed. From the analysis of the results, it was found that the initiation of cracking in the case of beams strengthened with 30 mm, 50 mm, and 70 mm layer depths occurred at 15.9 kN, 21.9 kN, and 24.9 kN, respectively.

Table 4 presents the numerical results for cracking and maximum load for various interface conditions and layer depths. The experimental values for the control beams and those strengthened with a 50 mm layer, with and without dowels, are also presented in the same table.

Table 4 indicates a good agreement between the experimental and numerical results for the cracking and maximum load. These results suggest that the interface conditions are crucial and significantly impact the strengthened beams' performance. A two-fold increment in both the cracking load and the maximum load was achieved with a monolithic connection. The use of dowels results in a behaviour similar to that of monolithic connection [23] and therefore significant enhancement of the load-bearing capacity of the strengthened elements can be achieved.

Based on the numerical results, the yield (My) and maximum (Mu) bending moment values for different interface condition assumptions and various layer depths were calculated, and the results are presented in Fig. 11.

As shown in Fig. 11, higher layer depths result in higher bending moment capacity. Also, a steeper increase in the bending moment capacity for increasing layer depth can be identified for a monolithic connection at the interface.

3.3. Design of strengthened elements: monolithicity coefficients

One of the most widely accepted methods for designing strengthened elements is using monolithicity coefficient values, which can be used to estimate the characteristics of strengthened elements based on the respective monolithic ones (Fig. 12).

Table 5 (Eqs. 1–4) defines the monolithicity coefficient factors [29].

For the calculation of monolithicity coefficient factors, numerical analyses were conducted for non-monolithic beams (coefficient of friction equal to 0.98 and cohesion equal to 1.8 MPa) and for the respective monolithic beams (perfect bonding at the interface) and Eqs. 1–4 were used. The monolithicity coefficient values for different layer thicknesses are presented in Table 6.

Fig. 13 presents the variation of coefficients Kk, kr, kθ,y and kθ,u for different layer depths.

As can be seen in Fig. 13, the coefficients are close to 1 (monolithic) for lower layer depths (30 mm). However, for higher depths, the performance of the strengthened members deviates significantly from monolithic behaviour. This indicates that for higher layer depths, the use of dowels may be necessary to provide enhanced bonding at the interface and a connection that approaches the monolithic.

3.4. Selection of UHPFRC characteristics

The properties of UHPFRC depend heavily on the material's tensile characteristics. Different fiber contents result in different tensile strengths and overall behaviour of the material. The selection of fiber content is related to parameters such as cost, the desired mechanical properties, and the ease of preparation and application of the material.

In strengthening applications, enhanced performance should be combined with ease of preparation and application of the material and good rheological properties. According to existing studies [2], strain hardening using steel microfibers can be achieved for fiber contents higher than 2 vol%. Therefore, it is suggested that fiber content higher than 2 vol% should be used. On the other hand, for fiber contents higher than 6 vol%, the workability of the material is very low, and the material cannot be prepared and applied easily [2]. Therefore, a suggested fiber content should be in the range of 2–6 vol%.

For the experimental investigation presented in the current study, a fiber content of 3 vol% was adopted, with a maximum tensile strength of 11.4 MPa and strain hardening behaviour (Fig. 7a). In the literature [2,4,41] higher fiber contents and higher tensile strengths have been reported.

In the present investigation, numerical analysis has been conducted, and the use of different tensile characteristics for the UHPFRC layers has been examined. The depth of the layers in all examined cases was 50 mm (similar to the experimental investigation), and different tensile strengths for the layers have been investigated, namely 11.5 MPa, 12.5 MPa, and 14 MPa. These values correspond to different fiber contents. In all the examined cases, strain-hardening behaviour and non-

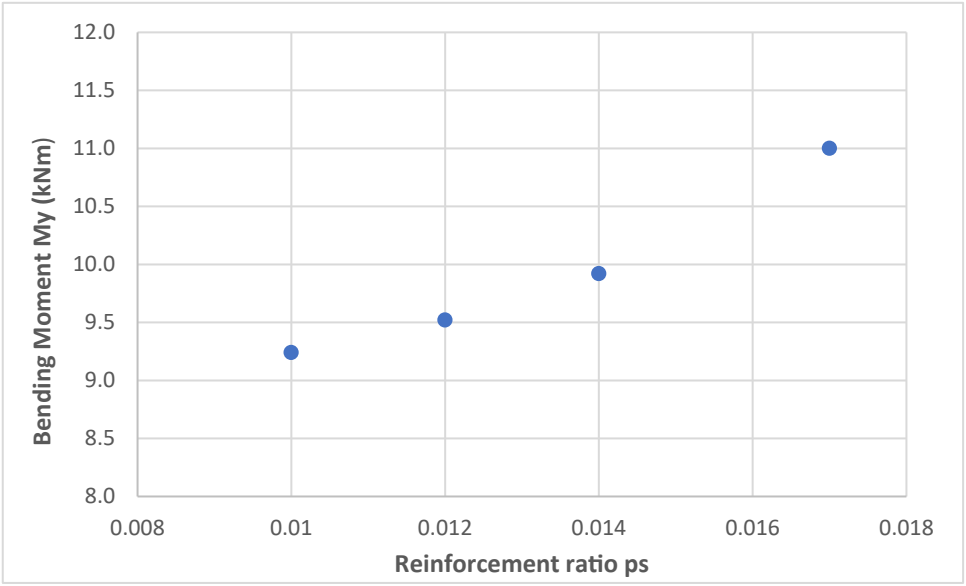

a)

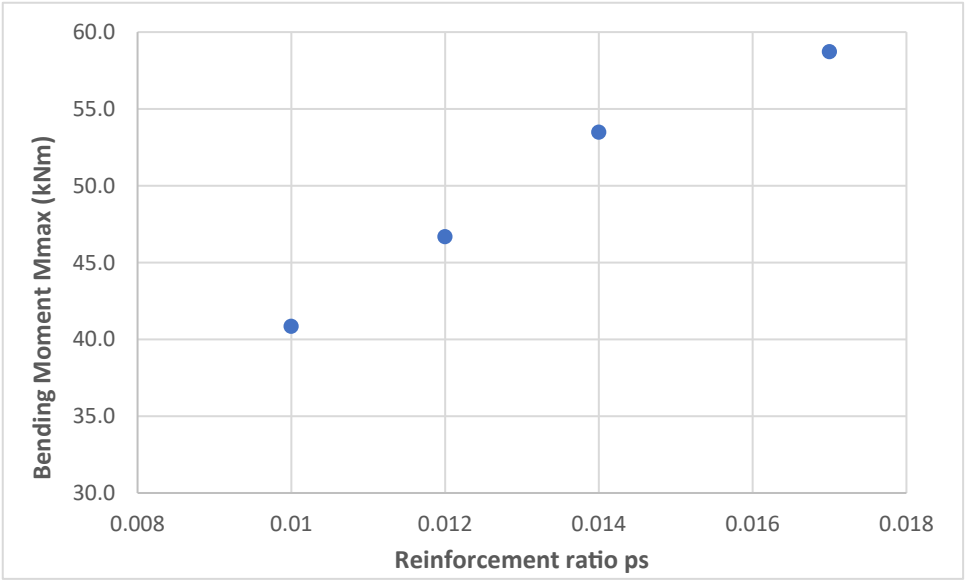

b)

Fig. 17. Bending Moment for different amounts of reinforcement at a) yield b) max.

monolithic behaviour have been assumed.

The numerical results for different tensile values are presented in Fig. 14.

From the results shown in Fig. 14, the load values at the end of the elastic phase and the maximum load were identified, and the results are presented in Table 7. In the same table, the values obtained from the experimental investigation are presented.

The results of Fig. 14 and Table 7 indicate that the tensile strength of the layer affects both the first cracking and the maximum load of the strengthened beams. The cracking load of the beams strengthened with a layer with a tensile strength of 11.5 MPa was increased by 53%, and the maximum load by 12.1%, compared to the control beam. For tensile strength of UHPFRC 12.5 MPa and 14 MPa, the cracking loads were increased by 71% and 85%, and the maximum loads by 17.9% and 20.8%, respectively.

The bending moment at yield (My) and the maximum (Mu) for the different tensile strength values are presented in Fig. 15.

From the results of Fig. 15, it is clear that the tensile strength of UHPFRC, which is mainly affected by the fiber content, is a parameter that should be considered when enhanced structural performance is required. However, this also affects the cost of the technique, and this aspect is examined in Section 4.

3.5. *Strengthening with UHPFRC layers and steel bars*

Steel bars in the UHPFRC layers should be considered for

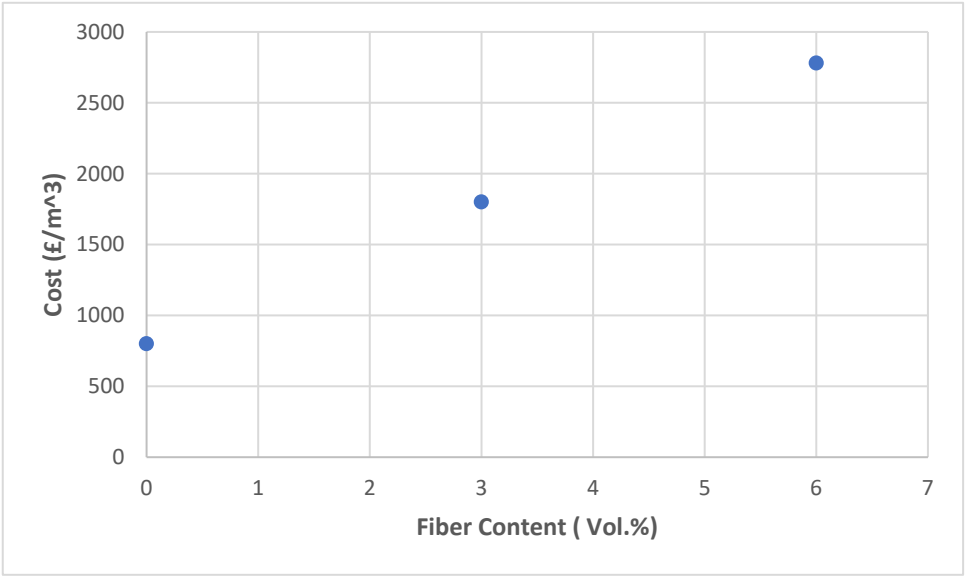

a)

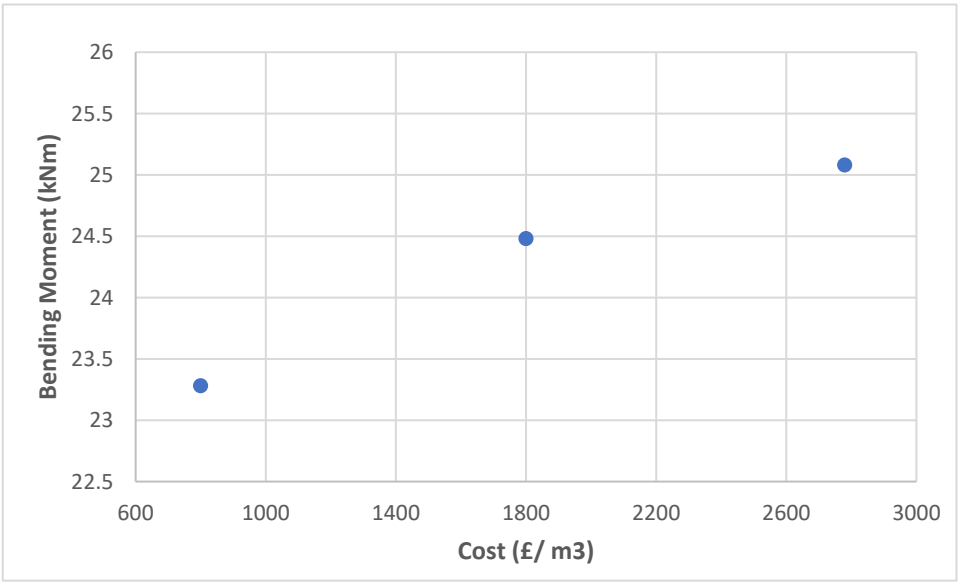

b)

Fig. 18. a) Cost per m^3 for different fiber contents b) Bending moment versus cost.

strengthening applications requiring high load-carrying capacity. In the present section, the performance of strengthened elements for different amounts of reinforcement is investigated.

Different amounts of reinforcement in the UHPFRC layer have been examined to investigate the effect of the amount of reinforcement on the performance of the strengthened members. In all the examined cases, the layer depth was assumed to be 50 mm and the properties of UHPFRC for 3 vol% were adopted (similar to the experimental investigation). Various diameters of steel bars were examined, and the results are presented in Fig. 16.

The cracking and maximum load were identified from Fig. 16, and the numerical results are presented in Table 8. This table also includes the average experimental load results.

From the results of Fig. 16 and Table 8, it can be seen that the use of UHPFRC layers without steel bars resulted in an increase of 53% in the cracking load and 12% in the maximum load. The addition of steel bars resulted in a significant increase in the cracking load and the maximum load. Therefore, the addition of two 10 mm, 12 mm, 14 mm, and 16 mm steel bars resulted in an increase of 131%, 138%, 148%, and 175%, respectively, in the cracking load and 97%, 124%, 158% and 183% respectively in the maximum load. From these results, it can be noted that when two steel bars with a diameter of 16 mm were used instead of the 10 mm bars, this resulted in an increase of 80% in the cracking load and 152% in the load-carrying capacity.

Apart from the load-carrying capacity, a slight increase in the stiffness of the strengthened beams was also observed. Therefore, the stiffness of the strengthened beams using 10 mm, 12 mm, 14 mm and 16 mm was calculated to be 28.7 kN/mm, 29.6 kN/ mm, 30.5 kN/mm and 31.6 kN/mm. In Fig. 17, the bending moment at yield (My) and at the maximum (Mu) for different reinforcement ratio ($\rho_s = A_s/bh$) are presented.

As can be seen in Fig. 17, an increase in the amount of reinforcement

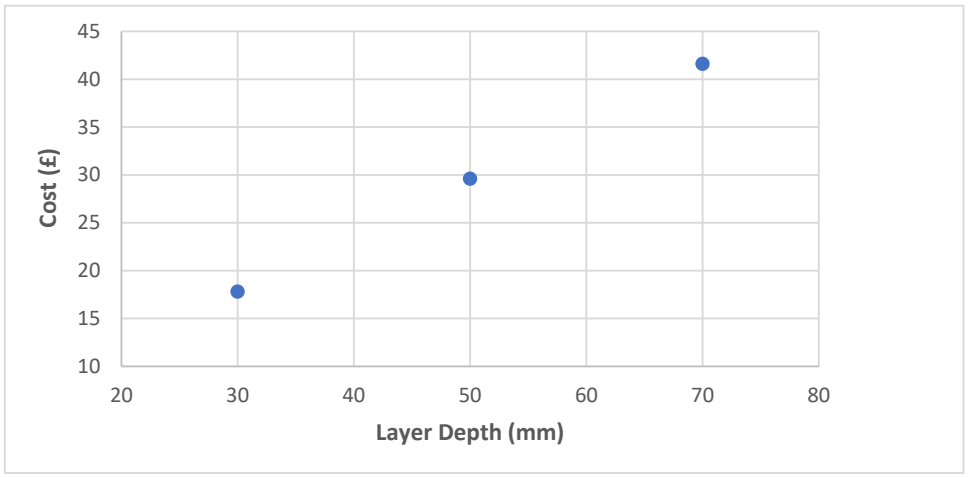

a)

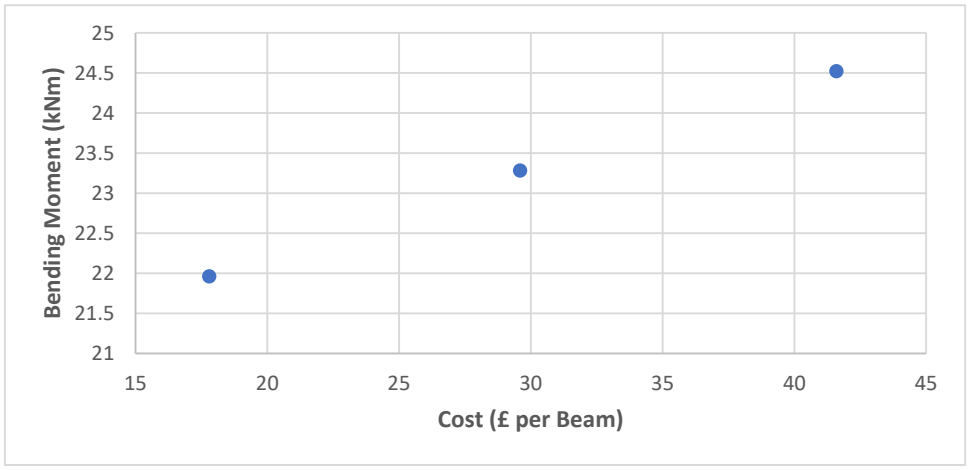

b)

Fig. 19. a) Cost for strengthening of 1 beam with different layer depths b) Cost in relation to bending moment.

results in a steep increase in the maximum bending moment. The addition of a 0.017 reinforcement ratio instead of 0.01 resulted in an increase of 19% in the yield moment and 44% in the maximum bending moment.

4. Discussion on the cost of materials and evaluation of the effect of key parameters

Based on the findings of the present study, adding UHPFRC layers without any extra reinforcement mainly increases the stiffness of the strengthened elements and results in a higher cracking load. This is also in agreement with other studies in the literature ([17], [22]). Based on existing studies ([2], [5], [41]), the mechanical properties of UHPFRC can be improved for higher fiber contents. This was also confirmed by the results of the present study and was reflected in the performance of the strengthened beams using higher fiber contents. Higher load-carrying capacity was achieved for the strengthened beams using UHPFRC layers with higher fiber contents. Other parameters affecting the performance of the technique are the layer depth, the level of preparation of the interface, and the incorporation of steel bars in the layers.

Crucial parameters that should be considered for the design of the examined technique are the required performance and the cost. Finding the optimum correlation between desired performance and cost is a challenging issue when applying a strengthening technique. UHPFRC has superior properties compared to other cementitious materials but is significantly more expensive. Incorporating a high volume of steel fibers, high-strength cement, fine silica sand, and superplasticizers significantly increases the material's cost.

The present section is focused on evaluating the materials cost for different strengthening configurations. It is worth mentioning that for the accurate calculation of the overall costs, additional parameters, such as labour costs and the costs of the required equipment, should be taken into consideration, which may vary from country to country for the examined techniques.

The approximate cost of the mix design of UHPFRC of the experimental investigation was calculated. Therefore, the cost of UHPC without fibers for the mix design of the experimental investigation and considering high quantities of high strength cement, silica sand, superplasticizer, silica fume, and GGBS, was estimated at approximately 800 £ /m^3. Commonly used fibers in UHPFRC are steel microfibers with a diameter of 0.16 mm and length 16 mm. These fibers were also used in the experimental investigation. The cost of these fibers is approximately 4.2 £ /kg. Therefore, the cost of UHPFRC using 3 vol% fibers is estimated at 1800 £ / m^3 and the cost of UHPFRC using 6 vol% fibers is 2780 £ / m^3.

Considering the cost of materials for strengthening one beam of the present investigation, an increase in the fiber content from 3 vol% to 6

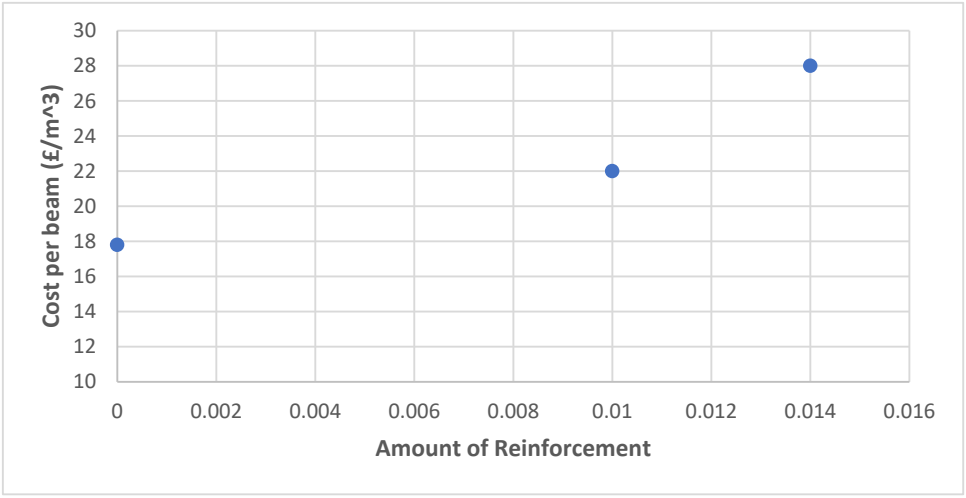

a)

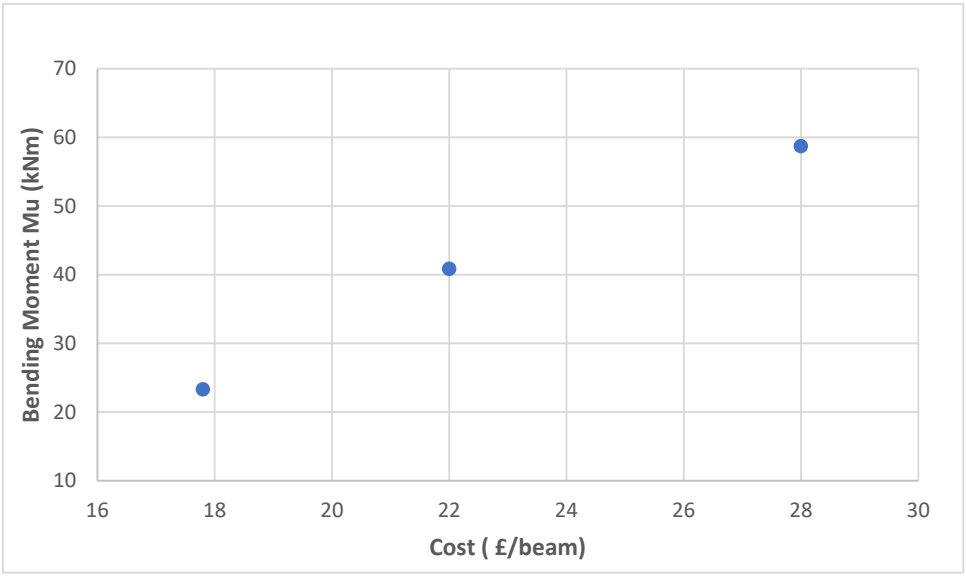

b)

Fig. 20. Cost for strengthening of 1 beam with different layer depths.

vol% results in a cost increase from 29.7 £ to 45.87 £ (54.4%). In Fig. 18a, the cost of UHPFC (per m^3) for different fiber contents is presented, while Fig. 18b shows the bending moment (Mu) in relation to the cost.

As shown in Fig. 18b, an increase of 2 kNm in the bending Moment capacity was achieved with an increase of 1980 £ /m^3 (or 248%) in the cost. This confirms that the cost of fibers should be considered when selecting the appropriate fiber content. However, it should be noted that the minimum required percentage of fibers to achieve strain hardening is approximately 2 vol% [2].

As presented in the previous sections, an alternative approach to increase the performance of the strengthened beams is to increase the layer depth. In the present section, the cost for strengthening one RC beam was calculated using different layer depths and 3 vol% fibers. The cost of the 30 mm layer depth was estimated at 17.8 £ , the cost of the 50 mm layer was 29.7 £ (an increase of 67%), and the cost of the 70 mm layer was 41.6 £ (a rise of 134%). The cost for the strengthening of one beam for the different layer depths is presented in Fig. 19a, and the bending moment increment in relation to the cost is presented in Fig. 19b.

Based on Fig. 19b, it can be noticed that an increase of 2.5 kNm in the bending moment using higher layer depths and the same fiber content (3 vol%) was achieved with a cost increase of 134%. On the other hand, increasing the fiber content and keeping the same layer depth resulted in a similar 2 kNm increase in the bending moment but at a higher cost increase of 248%.

In the present study, another approach to improve the performance of the strengthened beams involved adding steel bars in the UHPFRC layers. To evaluate the cost of this approach, the cost of incorporating varying amounts of extra reinforcement in the layers was calculated.

Incorporating two 10 mm steel bars in the 30 mm layer of the strengthened beam increased the cost from £ 17.8 to £ 22 (an increase of 24%). When 16 mm bars were added, the cost per beam rose to £ 28 (an increase of 57%). Fig. 20a presents the cost per beam in relation to the amount of reinforcement, while Fig. 20b illustrates the cost in relation to the bending moment.

Based on the results of Fig. 20, it can be noticed that an increase in the bending moment of 35 kNm, which was achieved with the incorporation of higher amounts of reinforcement, resulted in a 57% increase in the cost. Compared to the other approaches, the addition of extra reinforcing bars appears to be a more efficient method in terms of performance, and at the same time, the cost of materials is significantly lower.

Based on the present investigation the cost of UHPFRC is significantly increased with the fiber content. The cost of UHPFC without fiber is calculated at approximately 800 £ /m^3. The cost rises to 1000 £ /m^3 for 1 vol% and to 1800 £ / m^3 for 3 vol%. Considering a 50 mm layer depth, the respective cost per m^2 was 50 £ / m^2 and 90 £ / m^2. As presented in the present section, this cost further increases with the addition of steel bars. The cost of plain concrete for a typical C 30/35 class is approximately 150 £ /m^3 [42]. Of course, in the case of traditional methods using plain concrete, this cost rises significantly considering the cost of additional steel bars in the layers, dowels, and also labour costs. Alternative strengthening configurations include strengthening using TRMs. Based on studies [43], [44], [45] the cost of the technique may vary based on different configurations. Without considering labour costs, the cost of strengthening with the use of mortar, plastic connectors, and L shape GFRP results in a cost of 118 £ / m^2, while the cheapest solution using mortar, steel connectors, steel plate was 35 £ / m^2.

5. Conclusions

The selection of the appropriate fiber content, layer depth, and amount of reinforcement should be aligned with the required structural performance of the strengthening elements. When aiming for higher load-carrying capacity, adding steel bars in the layer is more effective in terms of performance compared to increasing fiber volumes or layer depths. The cost of materials is also significantly lower. Adding layers without any extra reinforcement increases mainly the stiffness of the elements, with the added advantage of easy application and lower labour costs. In addition, the reduction in the construction time of this technique should be considered.

Based on the results of the present study, the following conclusions can be drawn for the application of UHPFRC for strengthening purposes:

- Various methods can be employed to improve the performance of strengthened members using UHPFRC layers, including increasing fiber contents and layer depths, adding steel bars to the layers, and using dowels at the interface between UHPFRC and RC.
- Fiber contents ranging from 2-6 vol% are recommended for optimal performance and workability. The layer depths for conventional steel fibers, on the other hand, should range from 30-70 mm, considering factors such as the performance of the strengthened elements and the size effect.
- The interface connection between existing RC members and UHPFRC significantly affects the performance of strengthened elements, particularly for higher layer depths (>50 mm). Based on the results of the present study, a monolithic connection at the interface between UHPFRC and RC, which can be achieved with the use of dowels, resulted in a two-fold higher strength in both the first crack and maximum load stage as compared to a non-monolithic connection.
- Strengthening RC beams with UHPFRC layers with depths of 30 mm, 50 mm, and 70 mm and fiber content 3 vol%, enhanced their load-carrying capacity by 5.8%, 12.1%, and 18.1%, respectively.
- For monolithic connection at the interface, which can be achieved with the use of dowels, the load-carrying capacity of beams strengthened with 30 mm, 50 mm and 70 mm UHPFRC layers, and 3 vol% fiber content was increased by 11.8%, 18.1%, and 35.1%, respectively.
- Higher fiber contents and subsequently higher tensile strength resulted to higher load carrying capacity for the strengthened beam. Increment of the tensile strength from 11.5 MPa to 14 MPa led to enhancement of the load carrying capacity by approximately 8%.
- When applications require high load-carrying capacity and improved performance of strengthened members, the use of steel bars is a more effective option than higher layer depths and higher fiber contents in terms of both costs of materials and performance.
- The addition of 2 steel bars with diameters 10 mm, 12 mm, 14 mm and 16 mm in the UHPFRC layers resulted to an increase of the load carrying capacity by 97%, 124%,158%, 183%. When the primary target of the strengthening technique is to increase the stiffness of the strengthened members, it is recommended that UHPFRC layers without the use of steel bars should be used. This option should be the preferred one considering factors such as cost, ease of application, and construction time.
- Increment of the fiber content from 3 vol% to 6 Vo.% resulted in an increase in the cost of materials of 54.4%.
- An increase in the layer depth from 30 mm to 70 mm resulted in a 134% increase in materials costs.

Declaration of Competing Interest

The authors declare that they have no known competing financial interests or personal relationships that could have appeared to influence the work reported in this paper.

Acknowledgments

The authors would like to acknowledge Heidelberg Materials and Sika Limited for providing raw materials.

References

[1] Abbas S, Soliman AM, Nehdi ML. Exploring mechanical and durability properties of ultra-high performance concrete incorporating various steel fiber lengths and dosages. Constr Build Mater 2015;75:429–41.
[2] Paschalis S, Lampropoulos A. Fiber content and curing time effect on the tensile characteristics of ultra high-performance fiber reinforced concrete. Struct Concr 2017;18:577–88.
[3] Gesoglu M, Güneyisi E, Muhyaddin GF, Asaad DS. Strain hardening ultrahigh performance fiber reinforced cementitious composites: effect of fiber type and concentration. Compos B Eng 2016;103:74–83.
[4] Nicolaides D, Kanellopoulos A, Petrou M, Savva P, Mina A. Development of a new ultra high performance fibre reinforced cementitious composite (UHPFRCC) for impact and blast protection of structures. Constr Build Mater 2015;95:667–74.
[5] Kazemi S, Lubell AS. Influence of specimen size and fiber content on mechanical properties of ultra-high-performance fiber-reinforced concrete. Acids Mater J 2012;109:675–84.
[6] Paschalis SA, Lampropoulos A. Ultra high performance fiber reinforced concrete under cyclic loading. Acids Mater J 2016;113(4):419–27.
[7] Lampropoulos A, Nicolaides D, Paschalis S, Tsioulou O. Experimental and numerical investigation on the size effect of ultrahigh-performance fibre-reinforced concrete (UHFRC). Mater J 2021;14(19):5714.
[8] Mahmud G, Yang Z, Hassan A. Experimental and numerical studies of size effects of ultra high performance steel fibre reinforced concrete (UHPFRC) beams. Constr Build Mater 2013;48:1027–34.
[9] Awinda K, Chen J, Barnett S. Investigating geometrical size effect on the flexural strength of the ultra high performance fibre reinforced concrete using the cohesive crack model. Constr Build Mater 2015;105:123–31.
[10] Paschalis, S., Lampropoulos, A., Size Effect on the flexural performance of Ultra High Performance, Fiber Reinforced Concrete, HPFRCC-7 7th RILEM Workshop on High-Performance Fiber Reinforced Cement Composites, 1–3 June 2015, Stuttgart.
[11] Tsonos AD, Kalogeropoulos G. Analytical model for the design of HSFC and UHSFC jackets with various steel fiber volume fraction ratios for the retrofitting of RC beam-column joints. Sustainability 2021;13:11209.
[12] Tanarslan HM. Flexural strengthening of RC beams with prefabricated ultra high performance fibre reinforced concrete laminates. Eng Struct 2017;151:337–48.
[13] Lampropoulos A, Paschalis S, Tsioulou O, Dritsos S. Strengthening of reinforced concrete beams using ultra high-performance fibers reinforced concrete (UHPFRC). Eng Struct 2015;106:370–84.
[14] Dagenais M-A, Massicotte B. Cyclic behavior of lap splices strengthened with ultra high performance fiber-reinforced concrete. J Struct Eng 2017;143:04016163.
[15] Ramachandra Murthy A, Karihaloo BL, Priya DS. Flexural behavior of RC beams retrofitted with ultra-high strength concrete. Constr Build Mater 2018;175:815–24.

[16] Yin H, Teo W, Shirai K. Experimental investigation on the behaviour of reinforced concrete slabs strengthened with ultra-high performance concrete. Constr Build Mater 2017;155:463–74.
[17] Al-Osta M, Isa M, Baluch M, Rahman M. Flexural behaviour of reinforced concrete beams strengthened with ultra-high performance fiber reinforced concrete. Constr Build Mater 2017;134:279–96.
[18] Safdar M, Takashi Matsumoto T, Kakuma K. Flexural behavior of reinforced concrete beams repaired with ultra high performance fiber reinforced concrete (UHPFRC). Compos Struct 2016;157:448–60.
[19] Bruhwiler, E., Denarie E., Rehabilitation of concrete structures using Ultra-High Performance Fibre Reinforced Concrete, The Second International Symposium on Ultra High Performance, 2008, Kassel, Germany.
[20] Yoo D-Y, Oh T, Shin W, Kim S, Banthia N. Tensile behaviour of crack-repaired ultra-high performance fiber-reinforced concrete under corrosive environment. J Mater, Res Technol 2021;15.
[21] Elsayed M, Tayeh B, Elmaaty M, Aldahshoory A. Behaviour of RC columns strengthened with Ultra-High Performance Fiber Reinforced concrete (UHPFRC) under eccentric loading. J Build Eng 2022;47.
[22] Paschalis S, Lampropoulos A, Tsioulou O. Experimental and numerical study of the performance of Ultra High Performance Fiber Reinforced Concrete–Reinforced Concrete for the flexural strengthening of full scale members. Constr Build Mater 2018;186:351–66.
[23] Paschalis S, Lampropoulos A. Developments in the use of Ultra High Performance Fiber Reinforced Concrete as strengthening material. Eng Struct 2021;233:111914.
[24] Noor FA, Boswell LF. Small Scale Modelling of Concrete Structures. London: Elsevier applied Science Publishers Ltd; 1992.
[25] Tsioulou O, Lampropoulos A, Dritsos S. Experimental investigation of interface behavior of RC beams strengthened with concrete layers. Constr Build Mater 2013; 40:50–9.
[26] Lampropoulos A., Tsioulou O., Paschalis S., Dritsos S., Strengthening of Reinforced Concrete (RC) beams: RC versus UHPFRC layers, Iabse Congress, Resilient Technologies for Sustainable Infrastructure, 2–4 September 2020, Christchurch, New Zealand).
[27] Golias E, Zapris A, Kytinou V, Kalogeropoulos G, Chalioris C, Karayannis C. Effectiveness of the novel rehabilitation method of seismically damaged RC joints using C-FRP ropes and comparison with widely applied method using C-FRP sheets—experimental investigation. Sustainability 2021;13:6454.
[28] Chalioris C, Kosmidou PM, Papadopoulos N. Investigation of a new strengthening technique for RC deep beams using carbon FRP ropes as transverse reinforcements. Fibers 2018;6:52.
[29] Greek Organization for Seismic Planning and Protection, Greek Retrofitting Code (GRECO), Athens (in Greek); 2014
[30] Hellenic Technical Specification, Placement Dowels in Concrete Elements, Greek Ministry of Environment and Energy, 2009, (In Greek)
[31] BS 4449:2005 Steel for the reinforcement of concrete. Weldable reinforcing steel. Bar, Coil and Decoiled product. Specification, BSI, (2005)
[32] BS EN 12390–3:2009, Testing hardened concrete-Part 3: Compressive strength of test specimens
[33] BS EN 206:2013+A2:2021, Concrete. Specification, performance, production and conformity
[34] Konstadinidis AK. Earthquake Resistant Buildings From Reinforced Concrete, 2008. Pi-Systems International,; 2008.
[35] Murthy AR, Karihaloo BL, Priya DS. Flexural behavior of RC beams retrofitted with ultra-high strength concrete. Constr Build Mater 2018;175:815–24.
[36] Karayiannis C, Sirkelis. Strengthening and rehabilitation of RC beam–column joints using carbon-FRP jacketing and epoxy resin injection. Earthq Eng Struct Dyn 2008; 37:769–90.
[37] Aldahdooh MA, Bunnori NM, Johari MAM, Jamrah A, Alnuaimi A. Retrofitting of damaged reinforced concrete beams with a new green cementitious composites material. Compos Struct 2016;142:27–34.
[38] fib Bulletin No 55. Model Code 2010. Lausanne: International Federation for Structural Concrete, 2010
[39] Cervenka,V., Jendele, L., Cervenka, J., ATENA Program Documentation: Part 1 Theory, Prague, Czech Republic,2013.
[40] CEB Bulletin No. 213/214, CEB-FIP Model Code 90. International Federation for Structural Concrete, Lausanne, 2013
[41] Association Française de Genie Civil (AFGC), Ultra High-Performance Fiber Reinforced Concrete- Interim Recommendations, Bagneux, France, 2013
[42] Easy mix Concrete, Ready Mix Concrete Prices, available at https://www.easymixconcrete.com/, accessed on 3/10/23
[43] Furtado, A., Rodrigues H., Arêde, A., Varum, H., Cost-effective analysis of textile-reinforced mortar solutions used to reduce masonry infill walls collapse probability under seismic loads, Structures, 202, 28, 141–157.
[44] De Risi MT, André Furtado A, Rodrigues H, c, José Melo J, Verderame GM, António A, Varum H, Manfredi G. Experimental analysis of strengthening solutions for the out-of plane collapse of masonry infills in RC structures through textile reinforced mortars. Eng Struct 2020;207.
[45] Furtado A., Seismic vulnerability assessment and retrofitting strategies for masonry infilled frame buildings considering in-plane and out-of-plane behaviour PhD Thesis Portugal: Faculdade de Engenharia da Universidade do Porto, Universidade do Porto, Porto; 2020.